Electronic Supplementary Material (ESI) for Physical Chemistry Chemical Physics.

Supporting Information: The Physical Significance of the Kamlet-Taft π^* Parameter of Ionic Liquids

Nadine Weiß,[†] Caroline H. Schmidt,[†] Gabi Thielemann,[†] Esther Heid,[‡] Christian Schröder,[*,‡] and Stefan Spange[*,†]

†*Chemnitz University of Technology, Straße der Nationen 62, 09111 Chemnitz, Germany*

‡*University of Vienna, Faculty of Chemistry, Institute for Computational Biological Chemistry, Währingerstr. 17, A-1090 Vienna (Austria)*

E-mail: christian.schroeder@univie.ac.at; stefan.spange@chemie.tu-chemnitz.de

Contents

S1 Solvatochromic data and physico-chemical properties of the ionic liquids

The Kamlet-Taft parameter π^* obtained by the solvatochromic probe **Th** were reported in our previous work.[S1] Concerning the solvatochromic probe **DENA**, the π^* of [C$_n$mim]FAP (n=2,4,6) and [C$_4$mim]SCN were measured in this work.

Table S1: Kamlet-Taft π^* obtained by **DENA** in this work.

IL	$\widetilde{\nu}_{\mathrm{DENA}}$ $\frac{10^{-3}}{[\mathrm{cm}]}$	λ [nm]	π^*
[C$_2$mim]FAP	24.51	408	0.96
[C$_4$mim]SCN	23.87	419	1.15
[C$_4$mim]FAP	24.45	409	0.96
[C$_6$mim]FAP	24.39	410	0.98

A correlation between the Kamlet-Taft π^*-values measured *via* **DENA** and **BT** is given in Fig. S1.

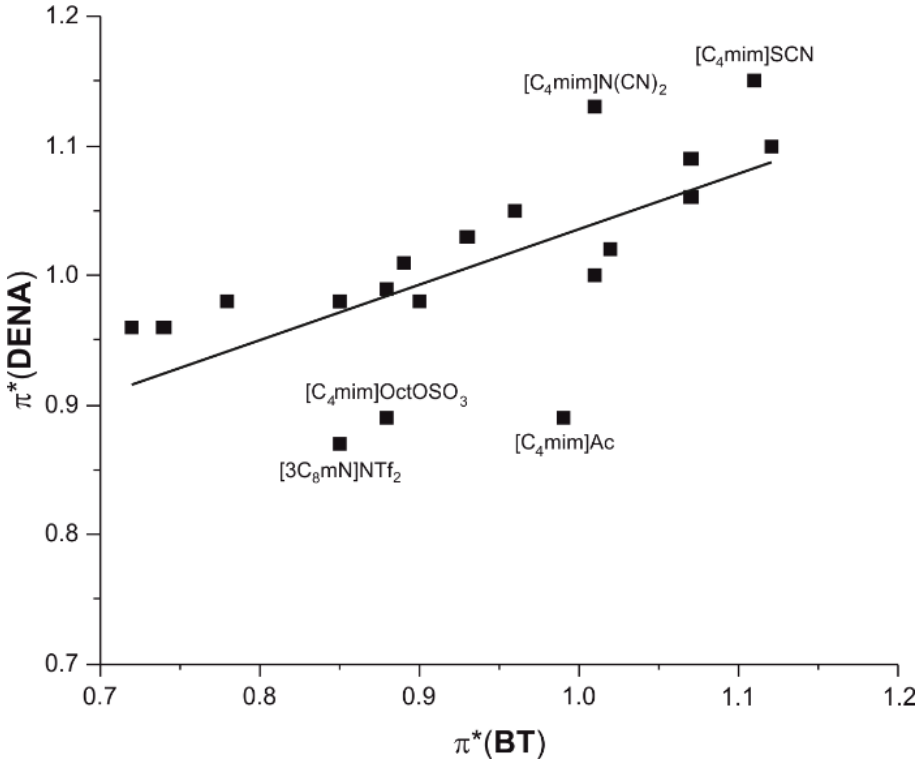

Figure S1: Correlation of the Kamlet-Taft π^*-values measured *via* **DENA** and **BT**.

The influence of water on the π^*-value is not strong as visible in Fig. S2-S5 which is in agreement with results from Baker *et al.*[S2]

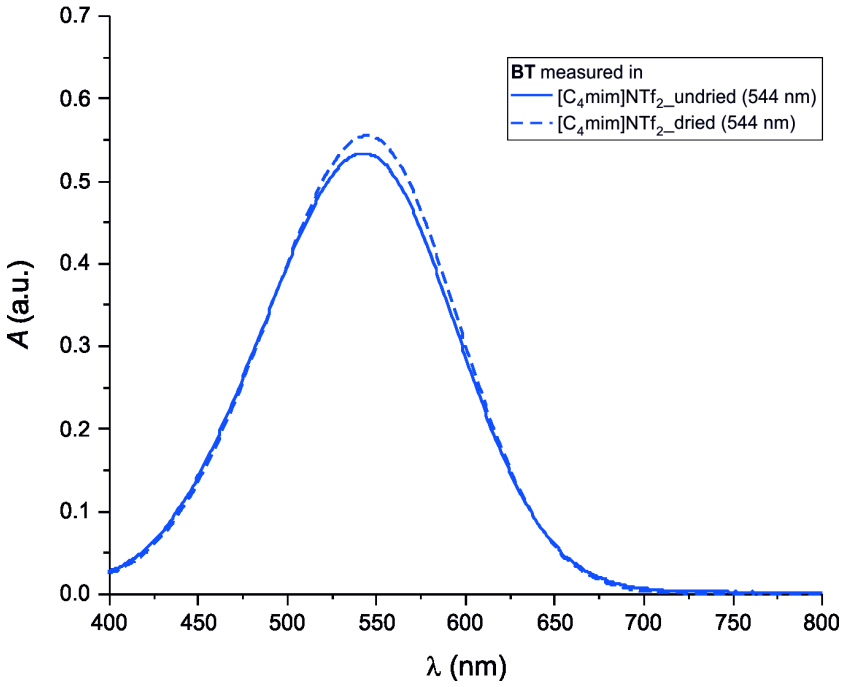

Figure S2: Absorption spectrum of **BT** in dried and undried $[C_4mim]NTf_2$.

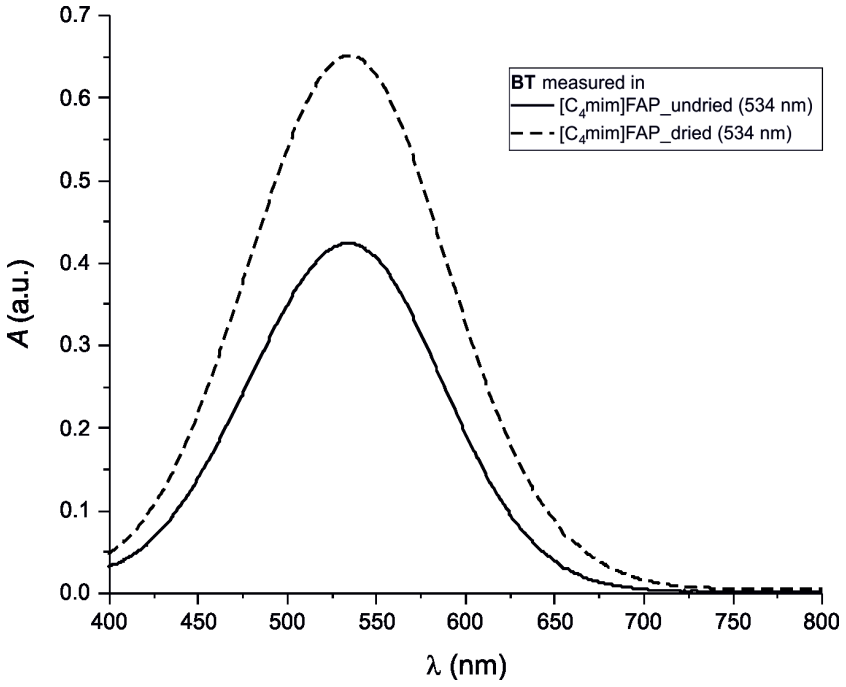

Figure S3: Absorption spectrum of **BT** in dried and undried $[C_4mim]FAP$.

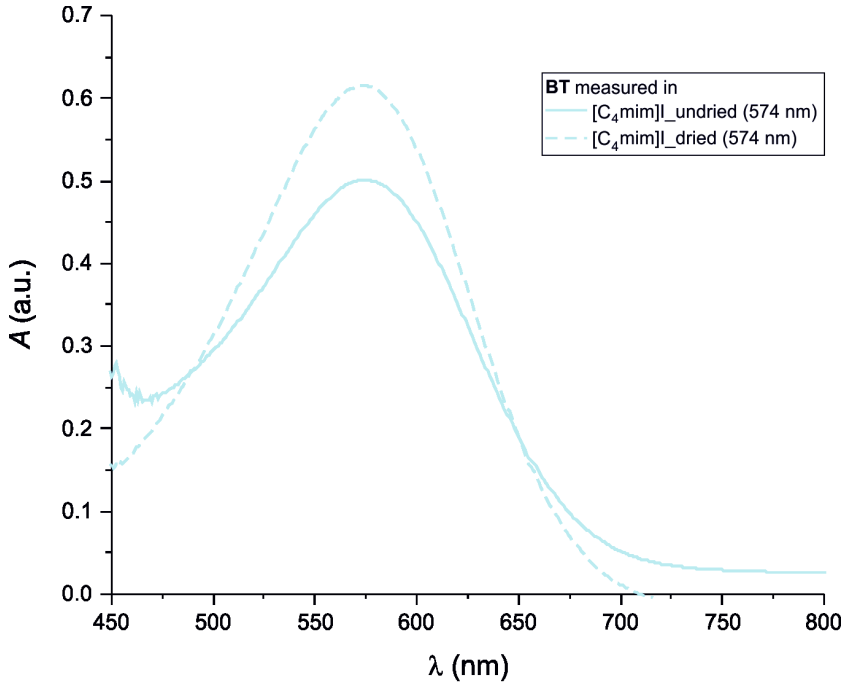

Figure S4: Absorption spectrum of **BT** in dried and undried $[C_4mim]I$.

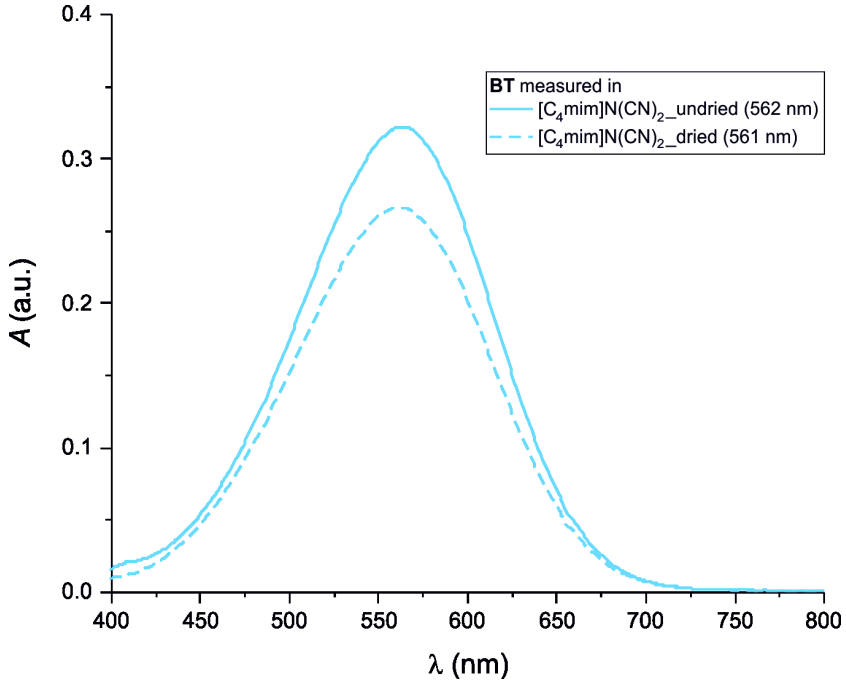

Figure S5: Absorption spectrum of **BT** in dried and undried $[C_4mim]N(CN)_2$.

Table S2 and S3 summarize all Kamlet-Taft π^* values used for the analysis of this work. The molar volume was evaluated from data of Ref. S3. The refractive indices of the IL can be found in Ref. S3–S7. The NMR-data of ^{129}Xe are taken from Ref. S8. The molecular polarizability volumes α_{QM} stem from the calculations described in Section S3. The references in the last column of Table S3 and S2 concern the Kamlet-Taft π^*-values obtained with the solvatochromic probe **DENA**.

Table S2: Kamlet-Taft π^* values derived from three different probes (**BT**, **Th** and **DENA**) as well as physical properties of the tetraalkylammonium-, tetraalkylphosphonium- and tetraalkylsufonium-based ionic liquids.

IL	$\widetilde{\nu}^{max}_{\mathrm{BT}}$ $\frac{10^{-3}}{[\mathrm{cm}]}$	π^*_{BT}	π^*_{Th}	π^*_{DENA}	V_m $[\frac{\mathrm{cm}^3}{\mathrm{mol}}]$	n_D	δ^{129}Xe [ppm]	α_{QM} [Å^3]	Ref.
$[3C_6C_{14}P]Cl$	18.08	0.93	0.93						
$[2C_2mS]NTf_2$	18.35	0.85	0.80					26.84	
$[3C_4mN]N(CN)_2$	17.89	0.99	0.99		259.1			32.31	
$[3C_4mN]CF_3CO_2$	18.02	0.95	0.93					30.59	
$[3C_4mN]NTf_2$	18.38	0.84	0.87		434.8			39.06	
$[3C_6mN]CF_3CO_2$	18.08	0.93						41.97	
$[3C_6mN]N(CN)_2$	17.99	0.96	0.98					43.69	
$[3C_6mN]NTf_2$			0.90		529.1			50.44	
$[3C_6mN]I$	17.83	1.01						42.77	
$[3C_8mN]CF_3CO_2$	18.22	0.89	0.86		476.2			50.37	
$[3C_8mN]N(CN)_2$			0.96		476.2			52.09	
$[3C_8mN]NTf_2$	18.35	0.85	0.84	0.87	657.9			58.84	S9
$[3C_{10}mN]CF_3CO_2$	18.15	0.91							
$[3C_{10}mN]N(CN)_2$	18.12	0.92							
$[3C_{10}mN]NTf_2$	18.35	0.85							

Table S3: Kamlet-Taft π^* values derived from three different probes (**BT**, **Th** and **DENA**) as well as physical properties of the imidazolium-based ionic liquids.

IL	$\widetilde{\nu}_{\mathrm{BT}}$ $\frac{10^{-3}}{[\mathrm{cm}]}$	π^*_{BT}	π^*_{Th}	π^*_{DENA}	V_m $[\frac{\mathrm{cm}^3}{\mathrm{mol}}]$	n_D	δ^{129}Xe [ppm]	α_{QM} [Å^3]	Ref.
[C_2mim]FAP	18.76	0.72	0.71	0.96	325.7		134.1	28.30	
[C_4mim]Cl	17.45	1.12	1.13	1.10	160.8		212.8	20.07	S10
[C_4mim]Ac	17.67	1.05	1.06	0.89	188.7		193.8	22.45	S11
[C_4mim]CH_3SO_3	17.76	1.02	1.04	1.02	188.0	1.477		23.73	S12
[C_4mim]OctylSO_3	18.25	0.88	0.96	0.89	326.8	1.471	171.9	37.02	S13
[C_4mim]I	17.42	1.13	1.13		178.6	1.572	250.7	22.88	
[C_4mim]CH_3OSO_3	17.83	1.01	1.05	1.00	207.5			24.08	S11
[C_4mim]CF_3CO_2	18.25	0.88	0.90	0.99	218.8	1.442		22.08	S14
[C_4mim]SCN	17.48	1.11	1.06	1.15	184.5		218.0	23.89	
[C_4mim]$N(CN)_2$	17.83	1.01	0.98	1.13	193.8	1.509	203.2	23.80	S15
[C_4mim]CF_3SO_3	18.22	0.89	0.90	1.01	220.8	1.437	171.9	23.66	S16
[C_4mim]BF_4	17.99	0.96	0.96	1.05	188.3	1.422	181.6	19.11	S16
[C_4mim]$C(CN)_3$	17.86	1.00	0.94				203.9	26.74	
[C_4mim]PF_6	18.08	0.93	0.90	1.03	208.3	1.409	173.5	20.69	S16
[C_4mim]NTf_2	18.35	0.85	0.83	0.98	291.5	1.427	158.2	30.55	S16
[C_4mim]FAP	18.69	0.74	0.78	0.96	358.4	1.379		32.11	
[C_4mim]NO_3			1.04		173.9	1.498		20.75	
[C_4mim]NO_2			1.05			1.509		20.27	
[C_4mim]ClO_4			0.98		190.5	1.473		21.95	
[C_6mim]Cl	17.61	1.07	1.06	1.06	194.9	1.515	206.6	23.87	S15
[C_6mim]Br	17.61	1.07	1.09	1.09	201.2	1.533	217.3	25.19	S15
[C_6mim]$N(CN)_2$			1.00		224.2	1.503		27.60	
[C_6mim]CF_3SO_3	18.18	0.90	0.92	0.98	255.1	1.441		27.46	S17
[C_6mim]BF_4			0.96		221.7	1.432		22.91	
[C_6mim]PF_6			0.93		240.4	1.417	177.7	24.49	
[C_6mim]NTf_2	18.35	0.85	0.86	0.98	326.8	1.430	162.1	34.35	S17
[C_6mim]FAP	18.59	0.78	0.80	0.98	393.7	1.382		35.91	
[C_6mim]NO_3			1.01		205.3	1.493		24.55	
[C_8mim]Cl	17.83	1.01	1.03		228.3	1.505	201.1	27.65	
[C_8mim]Br	17.76	1.02	1.04		235.3	1.523		28.97	
[C_8mim]I			1.07		228.3		221.9	30.46	
[C_8mim]$N(CN)_2$			0.97		257.7	1.499		31.38	
[C_8mim]CF_3SO_3			0.90		301.2	1.443		31.24	
[C_8mim]BF_4			0.93		255.1	1.433		26.69	
[C_8mim]PF_6			0.92		304.0	1.424	179.9	28.27	
[C_8mim]NTf_2			0.86		371.7	1.433	165.3	38.13	
[C_{10}mim]Cl	18.08	0.93	0.97		263.2	1.501	195.0	31.44	
[C_{10}mim]Br	17.95	0.97	1.00		268.8	1.515		32.76	
[C_{10}mim]$N(CN)_2$			0.96		288.2	1.495		35.17	
[C_{10}mim]BF_4			0.90		289.9			30.48	
[C_{10}mim]PF_6			0.89				181.5	32.06	
[C_{10}mim]NTf_2			0.86		395.3	1.436	168.4	41.92	

S2 Results for BT

As already mentioned in the main article, the fit results using the solvatochromic probe **BT** are similiar to those obtained by **Th**. They are summarized in Table S4. As the number of data points is significantly lower compared to **Th**, the Akaike and Bayesian Information criterion values are different and may only be used to compare correlations of physical properties with π^* measured by **BT**.

Table S4: Fit results using the solvatochromic probe **BT**. For the vertical oxidation potential ΔE_v only C_4mim based ILs were considered.

$\pi^* = f(\ldots)$	#IL	R^2	AIC	BIC
$\delta^{129}Xe$	17	0.89		
$1/V_m$	28	0.59	-62.4	-59.4
V_m	28	0.37	-50.4	-47.4
$1/V_m$, V_m	28	0.66	-64.7	-61.1
A_m	19	0.33	-33.8	-32.6
$1/A_m$	19	0.27	-32.0	-30.8
$\tilde{\alpha}_i$	34	0.16	-57.9	-54.1
A_m/V_m	19	0.81	-55.4	-54.1
V_m/A_m	19	0.78	-54.8	-53.6
n_D	19	0.79	-55.4	-54.2
ΔE_v	9	0.61	43.3	39.1

In Fig. S6 the Kamlet-Taft π^*-values measured by **BT** are depicted for the imidazolium based ionic liquids. This corresponds to the Fig. 5a in the main article. The dotted lines are the very same (orange: C_4mim based ILs, gray: C_6mim based ILs) as in the main article and obviously are also valid for the results obtained by **BT**. This demonstrates that π^*-values gained from the two solvatochromic probes **BT** and **Th** have a general meaning and do not depend on the structure of the probe.

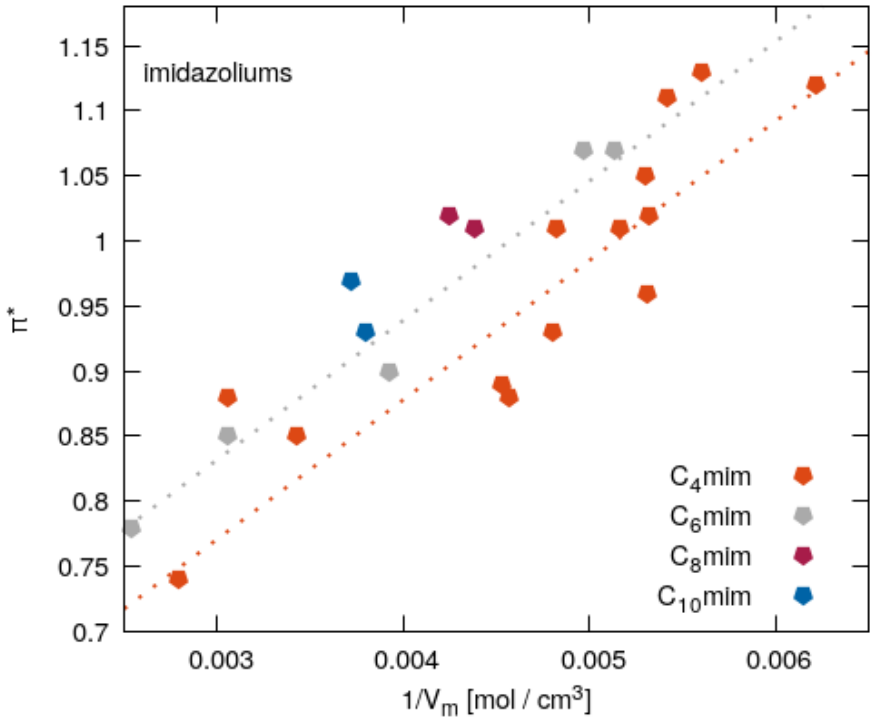

Figure S6: Kamlet-Taft π^*-values obtained by **BT** as a function of the inverse molar volume (which corresponds to the molar concentration.)

S3 Quantum-chemical calculations

The molecular polarizability volume $\widetilde{\alpha}$ and the dipole moment $|\vec{\mu}|$ of the ions were derived from RI-MP2 based calculations described in the methods section 3.3. As the ions are charged species, their molecular dipole moment is computed with respect to the center-of-mass of the corresponding ion. Both properties, $\widetilde{\alpha}$ and $|\vec{\mu}|$ are given in Table S5. Additionally, the vertical oxidation potential ΔE_V of some anions taken from Ref. S18 is stated.

Table S5: Molecular polarizability volumes $\widetilde{\alpha}$, molecular dipole moment with respect to center-of-mass $|\vec{\mu}|$ and the vertical oxidation potential[S18] of the ionic liquid ions.

Ion	$\widetilde{\alpha}$ [Å^3]	$\lvert\vec{\mu}\rvert$ [D]	ΔE_V [V]
Cl^-	4.53		1.99
Ac^-	6.91	4.14	1.48
$CH_3SO_3^-$	8.19	4.41	
I^-	7.33		
$CH_3OSO_3^-$	8.54	4.33	
$CF_3CO_2^-$	6.54	5.19	
SCN^-	8.35	1.54	2.22
$N(CN)_2^-$	8.26	0.95	2.86
$CF_3SO_3^-$	8.12	4.33	5.31
BF_4^-	3.57		6.35
$C(CN)_3^-$	11.2		2.78
PF_6^-	5.15		8.57
NTf_2^-	15.01	0.28	6.12
FAP^-	16.57	2.28	
NO_3^-	5.21		2.74
NO_2^-	4.73	0.77	
ClO_4^-	6.41		4.36
C_4mim^+	15.54	5.55	
C_6mim^+	19.34	10.31	
C_8mim^+	23.12	15.52	
$C_{10}mim^+$	26.90	20.98	

Although ΔE_V characterizes the oxidation potential of the anion and consequently the extreme case of completely removing the electron, we do not find a correlation between ΔE_V and the molecular polarizability volume as shown in Fig. S7.

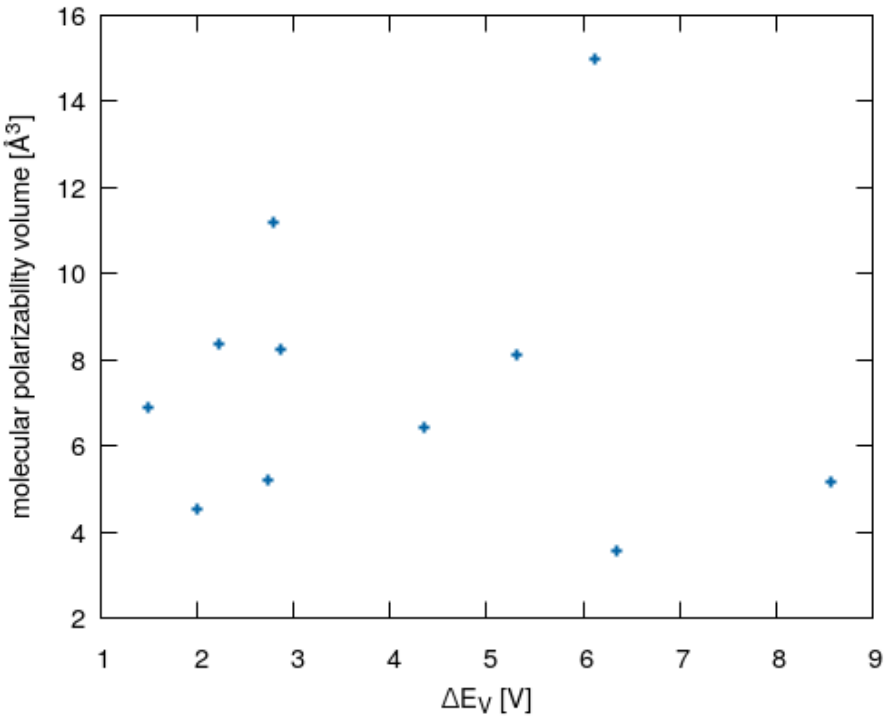

Figure S7: Molecular polarizability volume as a function of the vertical oxidation potential.

The molecular polarizability volume of the ionic liquid is simply the sum of the $\widetilde{\alpha}$ of the cation and the anion. These values are given in Table S2 and S3. Please note that these values are calculated in gas phase of single ions. Nevertheless, they show a strong linear correlation with the experimental molar volume V_m of Table S2 and S3 as shown in Figure 2 of the main article. The correlation has a R^2 of 0.91. This finding demonstrates that spatial heterogeneities which might be present in the ionic liquids play only a marginal role for the discussion on polarizability and polarity in this work.

S4 Taylor series of the Lorentz-Lorenz function

The Lorentz-Lorenz function is a function of the refractive index n_D and reads:

$$f_{LL}(n_D) = \frac{n_D^2 - 1}{n_D^2 + 2} = \frac{A_m}{V_m} \tag{1}$$

It is also the ratio between the molar refractivity A_m and molar volume V_m. This function can be approximated by a linear function obtained from a Taylor series at the expansion point $\langle n_D \rangle$=1.468:

$$f_{LL}(n_D) \simeq 0.278 + 0.51(n_D - 1.468) \tag{2}$$

The experimental data in Tables S3 and S2 correspond to the black triangles in Fig. S8. All these triangles are very close to the Taylor series in Eq. (2) plotted as dotted line. This indicates that the ratio in Eq. (1) is a linear function of the refractive index in the observed regime.

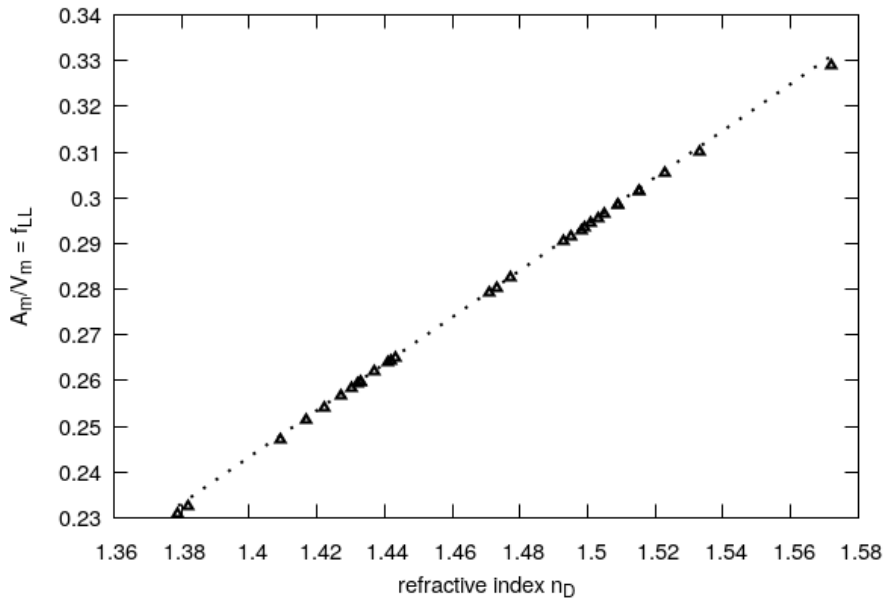

Figure S8: Experimental Lorentz-Lorenz function. The dotted line represents the Taylor series approximation in Eq. (2).

References

(S1) Spange, S.; Lungwitz, R.; Schade, A. *J. Mol. Liq.* **2014**, *192*, 137–143.

(S2) Baker, S. N.; Baker, G. A.; Bright, F. V. *Green Chem.* **2002**, *4*, 165–169.

(S3) Marcus, Y. *Ionic Liquid Properties from Molten Salts to RTILs*; Springer, 2016.

(S4) Seki, S.; Tsuzuki, S.; Hayamizu, K.; Umebayashi, Y.; Serizawa, N.; Takei, K.; Miyashiro, H. Comprehensive Refractive Index Property for Room-TemperatureIonic Liquids. *J. Chem. Eng. Data* **2012**, *57*, 2211–2216.

(S5) Fernádez, C. D. R.; Arosa, Y.; Algnamat, B.; Lago, E. L.; de la Fuente, R. *Phys. Chem. Chem. Phys.* **2020**, *22*, 14061–14076.

(S6) Lamas, A.; Brito, I.; Salazar, F.; Graber, T. A. *J. Mol. Liq.* **216**, *224*, 999–1007.

(S7) Hazrati, N.; M. Abdouss, A. A. M. B.; Pasban, A. A.; Rezaei, M. *J. Chem. Eng. Data* **2017**, *62*, 3084–3094.

(S8) Morgado, P.; Shimizu, K.; Esperanca, J. M. S. S.; Reis, P. M.; Rebelo, L. P. N.; Canongia Lopes, J. N.; Filipe, E. J. M. *J. Phys. Chem. Lett.* **2013**, *4*, 2758–2762.

(S9) Coleman, S.; Byrne, R.; Minkovska, S.; Diamond, D. *Phys. Chem. Chem. Phys.* **2009**, *11*, 5608–5614.

(S10) Ohno, H.; Fukaya, Y. *Chem. Lett.* **2008**, *38*, 2–7.

(S11) Doherty, T. V.; Mora-Pale, M.; Foley, S. E.; Linhardt, R. J.; Dordick, J. S. *Green Chem.* **2010**, *12*, 1967–1975.

(S12) Ab Rani, M. A.; Brant, A.; Crowhurst, L.; Dolan, A.; Lui, M.; Hassan, N. H.; Hallett, J. P.; Hunt, P. A.; Niedermeyer, H.; Perez-Arlandis, J. M.; Schrems, M.; Welton, T.; Wilding, R. *Phys. Chem. Chem. Phys.* **2011**, *13*, 16831–16840.

(S13) Jeličić, A.; Garcia, N.; H.G.Löhmannsröben,; Beuermann, S. *Macromolecules* **2009**, *42*, 8801–8808.

(S14) Tokuda, H.; Tsuzuki, S.; Susan, M. A. B. H.; Hyamizu, K.; Watanabe, M. *J. Phys. Chem. B* **2006**, *110*, 19593–19600.

(S15) Chiappe, C.; Pomelio, C. S.; Rajamani, S. *J. Phys. Chem. B* **2011**, *115*, 9653–9661.

(S16) Crowhurst, L.; Mawdsley, P. R.; Perez-Arlandis, J. M.; Salter, P. I. A.; Welton, T. *Phys. Chem. Chem. Phys.* **2003**, *5*, 2790–2794.

(S17) Mellein, B. R.; Aki, S. N. V. K.; Ladewski, R. L.; Brennecke, J. F. *J. Phys. Chem. B* **2007**, *111*, 131–138.

(S18) Jónsson, E.; Johansson, P. Electrochemical oxidation stability of anions for modern battery electrolytes: a CBS and DFT study. *Phys. Chem. Chem. Phys.* **2015**, *17*, 3697–3703.